

Mechanical Analysis of a Vertical Scanning System for 3D Images Acquisition with Microcontroller-based Electronic Design

J. Armando Segovia^{1,2}, Alberto Contreras² and Mayra P. Garduño²

¹National Institute of Nuclear Research (ININ)

Carr. Mexico-Toluca s/n, La Marquesa, Ocoyoacac, C.P. 52750. MEXICO

²Technological Institute of Toluca

Av. Inst. Tec. s/n, Metepec, Edo. de Mexico, C. P. 52140. MEXICO

armando.segovia@inin.gob.mx, albertoacs@prodigy.net.mx, mgarduño@hotmail.com

Abstract: - Herein are presented in detail the tasks that were developed to carry out a project that had as aim updating and improving the perception system of a Pioneer 3-AT mobile robot to enhance its navigation control by means of a mechanical system to let a laser range finder scanning and acquiring 2.5D and 3D images of the robot's environment. The system developed is a mechanism that is able to put in start position and to tilt automatically a laser range finder LMS200 with high precision, because the range of repetitive accuracy is very important to get good images. This precision was obtained with the aid of different parts that work together and with the best performance into its correspondent area; electronic area (control and communication circuits), mechanical area (stepper motor and mechanical design) and informatics area (acquisition and data processing). The system was developed to be an inexpensive device, using the most common elements, as a Microchip's microcontroller, which are easy to program and there are many models to choose the one that could fit our needs and budget, small elements and many job features, for example the PWM module, communication ports by USART and USB, and A/D channels, very important characteristics to control a stepper motor.

Key-Words: - 3D Scanner, Telemeter, Microcontroller, Navigation, mobile robot, Stepper Motor, LMS200 Laser Range Finder.

1 Introduction

The work described here is focused to develop a low cost navigation system, profiting from the existence of commercial devices, materials, parts and also using recycling materials.

There is a lot of techniques used to solve the problem of mobile robots navigation, and they depend on the use of different sensors, but to obtain good results, many times it is necessary to use two or more sensors concurrently.

For example, when a robot uses ultrasonic sensor, it can know only the distance to the obstacle. Same situation appears when it uses a light sensor, IR sensor, or point laser sensor, but with this configuration the robot can't identify what is the objects or, it needs specific characteristics to do it.

Other device widely used is the video camera, but with this one, colors (or intensity) and some other parameters as texture can only be detected, but determining the distance to the objects requires a lot of processing using two or more cameras. There exist many advantages to use range data provided by 3D laser range sensors, because is achieve a better accuracy of the object poses compared to stereo

camera solutions [1]; this is the main argument to use a laser range finder to obtain distances to the objects.

But the drawback of only 2D proximity information is that it may cause problems with overhanging objects (e.g. chairs, tables or stairways) [2].

The advantage of using a modified 2D range finder to generate 3D images is that it takes the distances and with them the robot can find and identify obstacles.

3D map building for mobile robots under cluttered indoor environments remains a challenge. The problem lies in two aspects: map consistency and computational complexity [3].

Vision is the most important source of information; this provides interaction with a 3D world. Also, if it would be possible providing to the machines with the same kind of vision, it could be possible that this perception model could be linked with a specified set of actions like identifying, grasping and avoiding objects, common tasks in the sensed 3D environment [4, 5].

This paper presents the principal problems and solutions proposed to create all the components that

assembled allowed built a 3D scanner using the Sick LMS200 (Fig. 1) existing in the Mobile Robotics laboratory of the Technological Institute of Toluca. To make an easier study and development of the system here described, the construction of the tilting system (TS) can be divided in three principal parts: mechanical, electronic, and programming part; they are described in following paragraphs.



Fig. 1. Telemeter laser range finder LMS200

2 Characteristics of the project elements

The project was developed in base of a 2D SICK telemeter laser range finder LMS200; the use of this device yields the advantage of scanning images with great exactly, fast, and high performance of distance measurement. To achieve this, two major principles of laser based distance measuring methods are used in industrial applications: Triangulation and time-of-flight (TOF). For active triangulation, the scene is illuminated by a laser source from one direction and viewed by a sensor from the other direction. The LMS200 operates by measuring the time of flight of laser light pulses: a pulsed laser beam is emitted and reflected if it meets an object. The reflection is registered by the LMS200 receiver. The time between transmission and reception of the impulse is directly proportional to the distance between the LMS200 and the object (time of flight). More or less TOF and phase measurement methods are long range technologies (over 1.0 meter) and triangulation based methods belong to close range methods [1].

The measurement data is available in real-time for further evaluation via the data interface [6], this data are transmitted to the host computer or the robot computer by the serial port RS232 or RS422.

In order to do that the TS could take 3D images, one box of 3mm aluminum was made (Fig.2). In this box the telemeter was mounted and it has the task of maintain the LMS200 over the pivot axis to do that the TS rotate around it, tilting and scanning one frame.

The main characteristics of the LMS200 are: field of view of 180° , operating range from 0 m to

80 m, 10 m of max range with 10 % reflectivity, possibility of different configuration in angular resolution at 0.25° , 0.5° or 1° , Systematic Error of 15 mm and Statistical Error 5 mm [7].

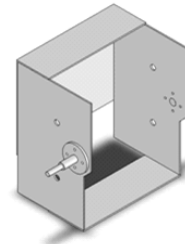


Fig.2. Box (turret) where the LMS200 is mounted.

The motion of the TS was developed with one stepper motor and one array of toothed pulley with a relation of movement of 1:2.5 and the main characteristics of the chosen motor are 3.5V/phase, 1.4A/Phase and 1.8deg/step .

The control of the TS was planed to use different elements, for example one microcontroller with at least one serial port communication, one PWM, one AD converter, so was elected the PIC16F870 as principal central control device, and as optional central control device one PIC18F2455 that has one USB port.

With this 3D scanner one can get images with a resolution of 0.36° or 0.72° per line in vertical direction, and one field of view of 180° on the horizontal.

3 Mechanical Part

3.1 Determining structure's center of mass and moment of inertia

The first activity was to determine the center of mass from the LMS200, and the box (turret) where the telemeter would be mounted (Fig. 3) to find the best point to put the pivot axis that would transmit the motion to the telemeter, creating in this way a new degree of freedom around "X" axis.

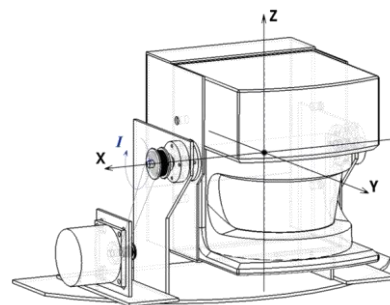


Fig. 3. Design of the TS and representation of the center of mass and the moment of inertia

The pivot must be placed on line with the coordinates that represent the position of the center of mass, it is very important in the design because it is the point where the motor will receive less stress.

In this activity the theory about center of mass and moment of inertia was used, to determine approximately the real position of this point characteristic.

Center of Gravity: The center of gravity is the point where the resultant weight of a particles system is concentrated [8, 9].

$$\bar{x} = \frac{\sum(x \cdot W)}{\sum W} \quad \bar{y} = \frac{\sum(y \cdot W)}{\sum W} \quad \bar{z} = \frac{\sum(z \cdot W)}{\sum W} \quad (1)$$

Where:

$\bar{x}, \bar{y}, \bar{z}$ represents the coordinates of the center of gravity of a particles system.

x, y, z represents the coordinates of each particle present in the system (centroid).

$\sum W$ is the sum of all the weights of all the particles in the system.

Center of Mass: The center of mass is the point where the mass from a particles system with a constant acceleration, for example the gravity, is concentrate at that point [8].

$$\bar{x} = \frac{\sum(x \cdot m)}{\sum m} \quad \bar{y} = \frac{\sum(y \cdot m)}{\sum m} \quad \bar{z} = \frac{\sum(z \cdot m)}{\sum m} \quad (2)$$

Where:

$\sum m$ is the sum of all the masses of all the particles in the system.

m is the mass.

The difference on these two terms that sometimes are interpreted as the same is that the second one is independent from the gravity force [8].

Another form to explain the relationship and difference of these terms is that the *center of mass of a particles system* is used when in the calculations the handling of the properties is related to the mass of the particles, and is used the *center of gravity* when the properties are associated with the weight of the particles [10].

Into the project it was necessary determining the center of mass because the properties that we knew were the mass and the density. The telemeter has a mass of 4.5 Kg and the turret was designed and made in aluminum that has a density of 2,700 Kg/m³.

The first step to determine the center of mass was to divide the telemeter and the turret in different regular figures to find the main characteristics of individual forms and then combine them into a composite figure (Fig. 4).

The second part of the project was to define a coordinate system to determine the exactly position

and dimension from every figure inside a space (Fig. 5).

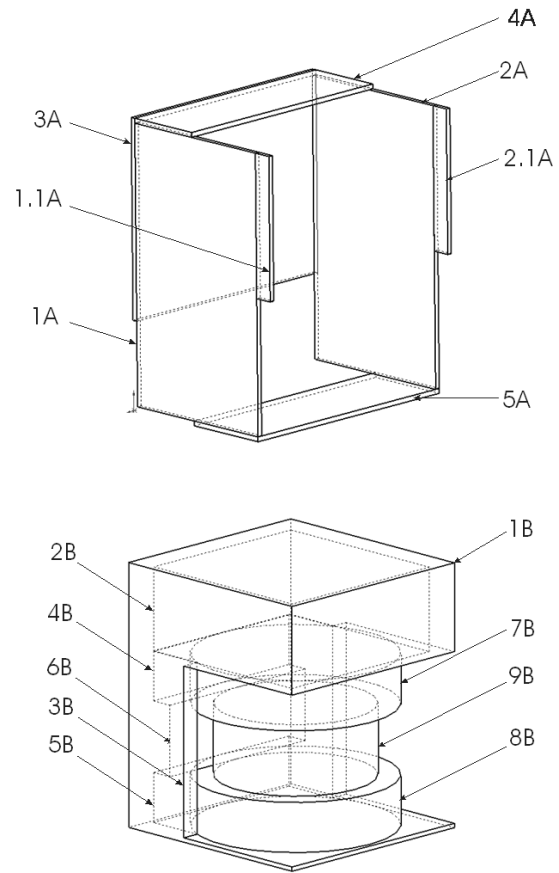


Fig. 4. Representation of the turret and telemeter LMS200 by regular geometric figures (2B, 3B, 4B, 5B and 6B are cutting extrusion).

Equations (8) to (10) and (13) to (15) were used to calculate the center of mass of each part, with this result also was determined the position where the pivot was placed in the turret by means of equation (2), with the purpose of decreasing the moment of inertia in the TS. The results are shown in Table I.

At this point it is important to define that this method isn't exact when the real distribution of mass is unknown, e.g. in the telemeter, but it can be approximated.

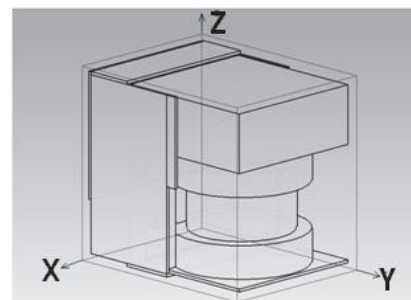


Fig. 5. Representation of the turret and telemeter inside of a coordinate system of reference to help calculate the position of the center of mass.

By the previous reason, it was necessary to make use of a complementary method to determine the center of mass, this was the experimental method (Fig. 6) where two or more points must be selected on the extremities of a object to use each of them as pivot to put in equilibrium the system and then trace a perpendicular line at the horizontal to determine the center of mass on the point where the lines intersect.

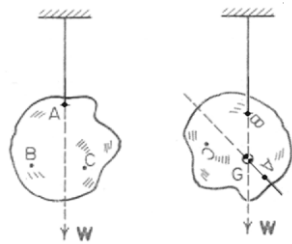


Fig. 6. Finding the center of mass in an irregular body or with irregular density distribution.

TABLE I

Position of the centroid of each regular figure that represent the turret and the LMS200, and the center of mass of the TS.

DESCRIPTION	COORDINATES INTO THE AXIS (mm)			MASS OF THE ELEMENTS (g)
	X	Y	Z	
Centroid of 1A	160.6	57.2	96.2	173.56032
Centroid of 1.1A	160.6	117.2	141.5	9.891072
Centroid of 2A	1.6	57.2	96.2	173.56032
Centroid of 2.1A	1.6	117.2	141.5	9.891072
Centroid of 3A	81.1	1.6	125.8	186.387264
Centroid of 4A	81.1	28.7	190.8	71.471808
Centroid of 5A	81.1	82.7	1.6	79.880256
Center of mass of the turret	81.1	44.17749811	104.1724939	704.642112
Centroid of 1B	81.1	132.2	95.7	17364.51983
Centroid of 2B	81.1	132.2	155.7	3960.335622
Centroid of 3B	81.1	158.45	66.2	7472.880675
Centroid of 4B	81.1	85.95	23.7	728.4729137
Centroid of 5B	81.1	85.95	108.7	728.4729137
Centroid of 6B	81.1	93.7	66.2	474.3577053
Centroid of 7B	81.1	136.2	23.7	174.0393484
Centroid of 8B	81.1	136.2	108.7	174.0393484
Centroid of 9B	81.1	135.7	66.2	151.9213033
Center of mass of the LMS200	81.1	108.0683195	101.2673993	4500
Center of mass of the TS	81.1	99.41831777	101.660712	5204.642112

After obtaining the center of mass and confirming the result, the next step was to determine the moment of inertia to know what type of motor is necessary to give movement to the mechanism.

The *moment of inertia* is a measure that gives the distribution reason of the mass in a particles system around one of its points [9]. In other words, it

represents the inertia to rotate that a body has, knowing that it is the resistance to the acceleration, in this case angular acceleration [11].

There are two ways to calculate the moment of inertia, doing the corresponding integrals (3) in all the volume of the body, or using the defined equations (4) to (7), (11), and (12), to be used in the regular bodies.

$$I = \int_m r^2 dm \quad I = \int_V r^2 \cdot \rho dV \quad (3)$$

$$I_{\bar{x}} = \sum (I_{\bar{x}} + D_I \cdot m) \quad (4)$$

Where:

I is the moment of inertia

r is the perpendicular distance between the spin axis and an arbitrary element dm . “the moment arm”.

ρ density

V volume

$I_{\bar{x}}$ is the moment of inertia into a composite figure, respect the spin axis “ \bar{x} ” that crosses the center of mass.

$I_{\bar{x}}$ is the moment of inertia of each figure that composes the composite figure with respect to their spin axis “ \bar{x} ”, which crosses their centroid.

D_I is the distance between the “ \bar{x} ” axis and “ \bar{x} ”, in each regular figure that form the composite figure.

As well as there are equations to calculate the area and volume also are defined equations to calculate the moment of inertia and the centroid in the regular geometric figures, as follow.

$$I_{\bar{x}} = \frac{1}{12} m(b^2 + c^2) \quad (5)$$

$$I_{\bar{y}} = \frac{1}{12} m(c^2 + a^2) \quad (6)$$

$$I_{\bar{z}} = \frac{1}{12} m(a^2 + b^2) \quad (7)$$

$$\bar{x} = \frac{a}{2} + \Delta x \quad (8)$$

$$\bar{y} = \frac{b}{2} + \Delta y \quad (9)$$

$$\bar{z} = \frac{c}{2} + \Delta z \quad (10)$$

$$I_{\bar{x}} = I_{\bar{y}} = \frac{1}{12} m(3 \cdot r^2 + L^2) \quad (11)$$

$$I_{\bar{z}} = \frac{1}{2} m \cdot r^2 \quad (12)$$

$$\bar{x} = C_x \quad (13)$$

$$\bar{y} = C_y \quad (14)$$

$$\bar{z} = \frac{L}{2} + \Delta z \quad (15)$$

Where:

$I_{\bar{x}}, I_{\bar{y}}, I_{\bar{z}}$ are the moment of inertia around the axis indicated on the subscript.

a, b, c are the width (on axis X), length (on axis Y) and high (on axis Z) respectively in a prism.

$\Delta x, \Delta y, \Delta z$ are the displacement that the figure has respect the center of the coordinate system.
 r, L are the radius and length respectively in a cylinder.

C_x, C_y are the coordinates center of the circular face on a cylinder.

For practical cases the use of regular figures that form a composite figure is most usual and fast [8].

The following stage of the project was find the moment of inertia of the turret and the telemeter, it was calculated with the aid of the regular figures that compose the system and the equations (5) and (11) corresponding with each figure that define the turret and the telemeter considering the same coordinate system (Fig. 5), to obtain later the moment of inertia of the whole system using equation (4), getting the results shown in Table II.

It's important once again notate that the use of this method isn't exact when the real mass or density distribution is unknown, but it will be approximated to the real value if the center of mass is correctly calculated.

TABLE II

Moment of inertial (I) of each regular figure that represent the turret and the LMS200, and the moment of inertial of the TS.

ELEMENT	Moment of inertial (g·mm ²)	Moment of inertial (kg·m ²)	D _i (mm)
1A	669075.0336	0.000669075	111.9208649
1.1A	7620.378601	7.62038E-06	183.7337476
2A	669075.0336	0.000669075	111.9208649
2.1A	7620.378601	7.62038E-06	183.7337476
3A	274909.4099	0.000274909	125.8101745
4A	15552.50366	1.55525E-05	192.9464433
5A	21695.7438	2.16957E-05	82.71547618
1B	84740303.81	0.084740304	163.2033394
2B	6899234.681	0.006899235	204.2531028
3B	15638403.98	0.015638404	171.7231566
4B	178915.9829	0.000178916	89.15768335
5B	178915.9829	0.000178916	138.5752233
6B	125546.6727	0.000125547	114.7263265
7B	237099.6056	0.0002371	138.2466274
8B	237099.6056	0.0002371	174.2588018
9B	148639.1701	0.000148639	150.9865226
TS	64692782.91	0.064692783	

Knowing that the concept of *moment of inertia* in a rotational movement and the *inertial mass* in a linear movement are analogous [11], and making use of the second law of Newton, it is easy to calculate by means of equation (16) the required torque to move the telemeter and the turret, knowing

that the moment of inertia of the system is 0.064692783 Kg·m² and that the required max angular acceleration is 2.61799 rad/s², the reason of this value is explained in section 2.2.

$$\tau = I \cdot \alpha \quad (16)$$

$$k = \sqrt{I/m} \quad (17)$$

Where:

τ is the torque generated by an angular acceleration and a moment of inertia, doing analogy to the second law of Newton in a rotational movement.

α is the angular acceleration of a body (rad/s²)

k is the radius of spin

In summary, the important data to the design were the exactly position of the center of mass, which is on the coordinate point (81.1, 99.42, 101.66) mm respect the coordinate system of reference (Fig.5), and the moment of inertia of the TS in that point, which has a value of approximate 0.0647 kg·m².

3.2 Motor and power transmission system

Other important part into the mechanical design is the generation of movement and the transmission of it. One relevant step into the election of the system of movement is identifying and defining what will be the input and the output from the mechanism, for example in this case we needed as input and output a rotational movement, with high rate of repetitive accuracy.

There are many methods to approve these two principal characteristics, for example using one gear box or a pulley system (Fig. 7).

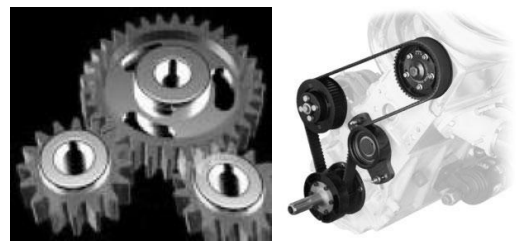


Fig. 7. Some elemental mechanisms to transmit and generate movement in one machine.

So, the selected power transmission system was a mechanism of toothed pulleys and its respective synchronous belts type PowerGrip Timing moved by a stepper motor. This system was chosen because it's easy to build and it has excellent physics characteristics, for example, it works as a gear box but with the advantage that with the belt, the driving pulley and the driven pulley can be put at different distance.

To determining the principal dynamic behavior of the pulley arrange, it was calculated by means of equation (18) and (19), where the angular speed is inversely proportional to the relation of pulleys, and the torque conduction is directly proportional to the relation of pulleys.

$$\frac{\omega_{in}}{\omega_{out}} = \frac{N_{out}}{N_{in}} \Rightarrow \omega_{out} = \omega_{in} \cdot \left(\frac{N_{in}}{N_{out}} \right) \quad (18)$$

$$\frac{\tau_{in}}{\tau_{out}} = \frac{N_{in}}{N_{out}} \Rightarrow \tau_{out} = \tau_{in} \cdot \left(\frac{N_{out}}{N_{in}} \right) \quad (19)$$

Where:

$\omega_{in}, \omega_{out}$ are the angular speed of the driving pulley and the driven pulley respectively.

τ_{in}, τ_{out} are the torque in the driving pulley and the driven pulley respectively.

N_{in}, N_{out} are the number of teeth of each pulley, the driving pulley and the driven pulley respectively.

The driving pulley of the mechanism has 16 teeth with a step of 0.080 inches and the driven pulley has 40 teeth with the same step, with these data we can define the relation of movement in a scale of 1:2.5.

The selected motor is a stepper motor because the handling of the position is easy and the precision only depends of the step angle of the motor. The main characteristics of the chosen motor are (as mentioned before): 3.5V/phase, 1.4A/Phase and 1.8deg/step.

In order to assure that the motor could be able to support the load, it was put experimentally under a torsion test using a mass of 2 Kg. placed at a distance of 1cm from the motor's shaft and using a work frequency of 208 Hz to produce a speed rotation around 62.4 RPM, because this is the needed to generate around 25 RPM (150°/s) of speed rotation on the telemeter LMS200 as in the 3-D Sweeping Laser Range-Finder commercial model.

The result of the test was satisfactory obtaining a torque of 0.1962 N·m (27.78oz-in) in the motor and in the driven pulley a torque of 0.4983 N·m (70.55 oz-in) that is more than the torque necessary to move the telemeter, which was calculated using (16) obtaining 0.1694 N·m (23.98 oz-in).

4 Electronic Part

The second part of the development of the TS had as objective designing the circuit and the printed

circuit board (PCB) to control the mechanism (figures 8 and 10), where to get the best results, it was divided into three general parts: control system, communication and power circuit, all of them have a specific job into the design as described in the subsections below.

4.1 Control System

This section is composed by two important integrated circuits, the U4 and the U5 (Fig.8 and Fig. 10), the first is the PIC16F870 microcontroller, who has the job to identify and generate the different signals to produce the correct performing of the motor.

Microcontroller lets modify and control direction, step clock, half/full step selection, and enable/disable phase power using the serial communication. It also communicates with the computer to receive the able commands to control the whole mechanism.

The microcontroller works with a 4 MHz crystal oscillator, obtaining 1μs machine cycle time (T_{MC}); with this T_{MC} the microcontroller can be configured to do that the serial port works at a speed until 62.5K bauds and with this can be increase the speed to send and receive the commands and info about the present line of the scan in which the telemeter is on.

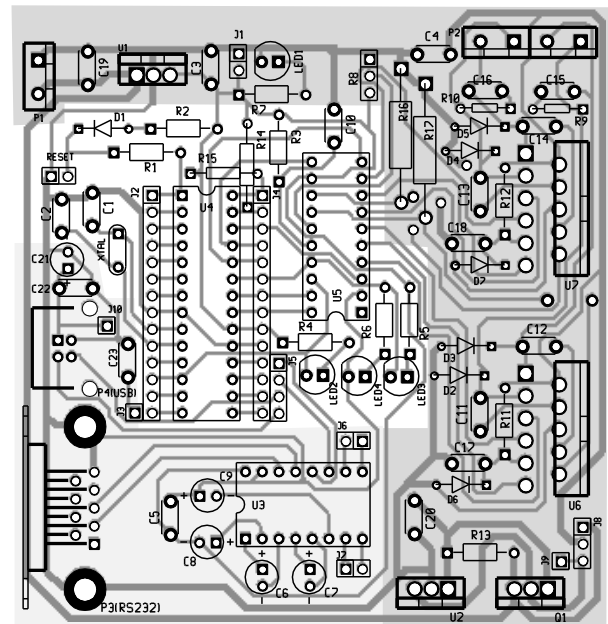


Fig.8. Design of the PCB used to control the TS. Where the light gray is the communication system, the white area is the control system, and the dark gray zone is the power supply circuit.

Also the design of the PCB has the plus that it can be upgraded to use the USB port to the

communication; it was made thus because the tendency of the technology is eliminating the COM port in the computers and replace it with the USB port.

This upgrade is easy to do, only adding three capacitors C21, C22 and C23 and one USB port (Fig. 8) following the USB connection schematic (Fig. 9) that is based in the Microchip PIC18F4550 USB Prototyping Board (PIC-USB-4550), in addition changing some bridges and replacing the microcontroller PIC16F870 with the PIC18F2455, that has a USB port. The most significant difference of these two microcontrollers is that the first belongs to the family of midrange microcontrollers and the second one is from the family of high-range microcontrollers [12].

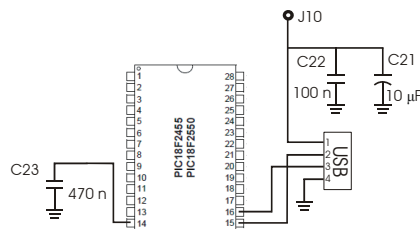


Fig.9. USB connection schematic to the PIC18F2455.

The bridges that are necessary to change to make the upgrading, are: the two bridges that are near of the PIC's socket, in front of the 17 and 18 pins, they need to be moved to the pins that are in front of the 15 and 16 socket's pins, as well place one more bridge in the pin in front of the 14 socket's pin.

The other integrated circuit is the L297 who is a stepper motor controller which is commanded by the signals coming from the PIC16F870. It produces the signals sequence needed to drive the stepper motor [13, 14], these signals are shown in Table III if it's working at full step or in Table IV when working at half step.

TABLE III

Signals required to move the stepper motor at full step

STEPP	CABLE A	CABLE B	CABLE C	CABLE D
1ST TIME	+ Vcc	GND	+ Vcc	GND
2TH TIME	+ Vcc	GND	GND	+ Vcc
3TH TIME	GND	+ Vcc	GND	+ Vcc
4TH TIME	GND	+ Vcc	+ Vcc	GND

TABLE IV

Signals required to move the stepper motor at half step

STEPP	CABLE A	CABLE B	CABLE C	CABLE D
1ST TIME	+ Vcc	GND	+ Vcc	GND
2TH TIME	+ Vcc	GND	GND	GND
3TH TIME	+ Vcc	GND	GND	+ Vcc
4TH TIME	GND	GND	GND	+ Vcc
5TH TIME	GND	+ Vcc	GND	+ Vcc
6TH TIME	GND	+ Vcc	GND	GND
7TH TIME	GND	+ Vcc	+ Vcc	GND
8TH TIME	GND	GND	+ Vcc	GND

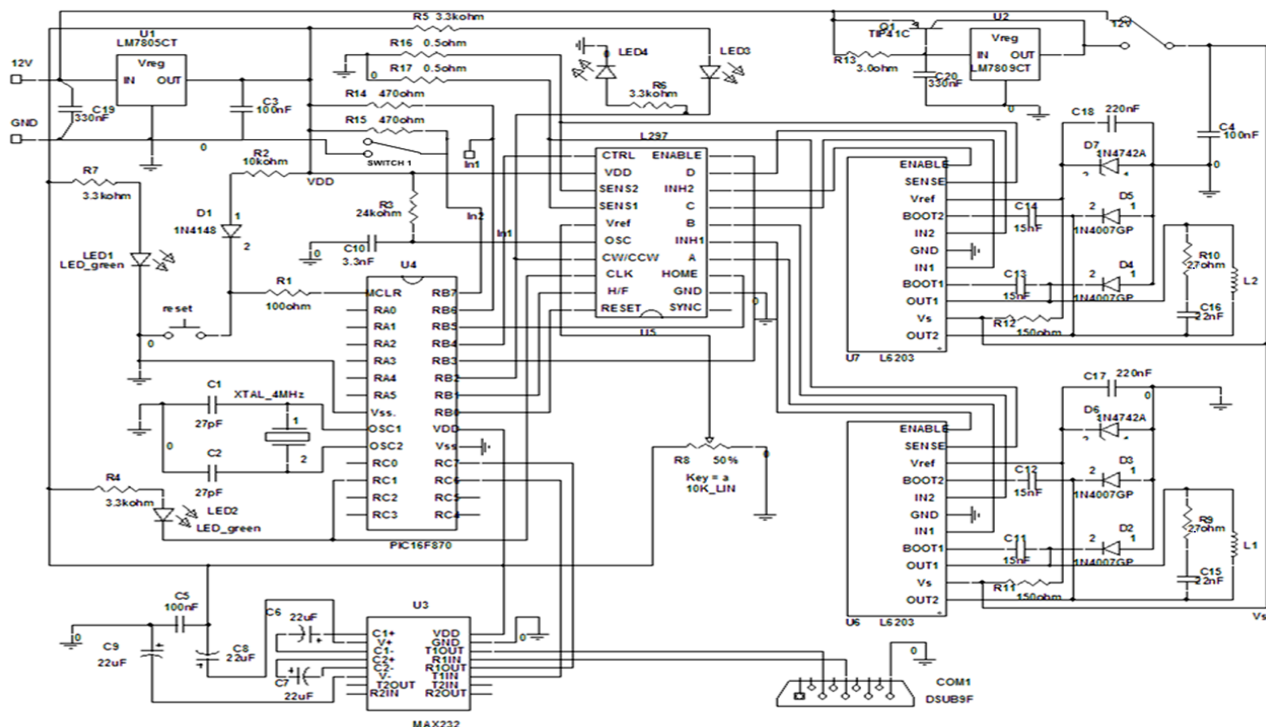


Fig.10. Electronic diagram designed for TS, to control a stepper motor with a computer using a PIC16F870.

The advantage of using one stepper motor controller is that with this one the microcontroller has an additional protection of the parasite currents that may come from the stepper motor's phase. Also with this element it is possible to have better control of the motor only sending the needed and minimal signals from the PIC.

4.2 Communication

This part of the circuit is very important and necessary because through it the user will be able to configure and to know the state of the system by means of the serial port of a computer.

This section has the goal to communicate the microcontroller with the host computer, where the user can interact with the system.

The microcontroller has the mission of receiving the control data to manage the TS and transmitting information about its status; depending of which microcontroller is used it could be possible use the serial port RS232 or the USB port.

The PIC16F870 has one Universal Synchronous Asynchronous Receiver Transmitter (USART) module also known as a Serial Communications Interface or SCI [15].

One special characteristics of the USART is that it can be configured as a full duplex asynchronous system that can communicate with peripheral devices, such as personal computers (PC), or it can be configured as a half-duplex synchronous system that can communicate with peripheral devices, such as A/D or D/A integrated circuits or serial EEPROMs.

But getting communication with the computer the microcontroller needs one interface that transforms the signals of the PIC at the appropriated levels for the PC.

In this application we use a standard MAX232 as the interface between the PC and the PIC16F870, to transform the TTL signals (0-5V) from the microcontroller to RS-232 signals ($\pm 12V$) used by the COM port of the computer and vice versa.

The communication was configured to 9,600 bauds, 8 data bits and 1 stop bit being the standard values, but to improving performance can be configured until 62,500 bauds.

To design the communication sector of the PCB was used the electronic diagram, that is showed in the MAX232's data sheet documentation (Fig. 11).

4.3 Power Circuit

In the power circuit the correct election of a motor's drive was more exhaustive, because if in the design

is used a circuit with low characteristics, it may cause damage or bad work of the motor and the full-bridge driver.

Determining which of the commercial drivers has the characteristics indicated to the job, it was necessary to use equations (21) to (22) with the characteristics of the motor as the current needed to obtain the appropriated torque to move the telemeter and the turret, and the desired max rotation speed.

$$power(W) = \frac{2\pi * [torque(N \cdot m)] * [rotation\ speed(rpm)]}{60} \quad (20)$$

$$power(W) = [voltage(V)] * [current(A)] \quad (21)$$

$$current(A) = \frac{power(W)}{voltage(V)} \quad (22)$$

With the results obtained, we chosen the L6203, which has appropriated ratings of voltage and current to work, high switching speeds, protection systems, thermal shutdown and limit current sensor.

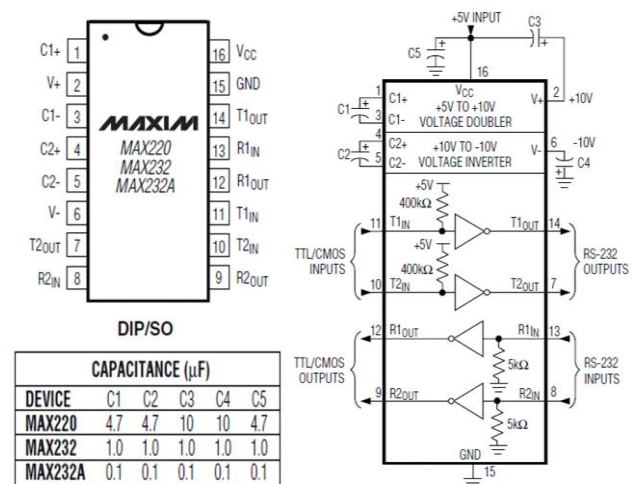


Fig. 11. MAX232/MAX232A Pin Configuration and Typical Operating Circuit (courtesy of Maxim Integrated Products).

The configuration of the L6203 to do it work at a supply voltage range between 9V-12V was made using the datasheet documentation [18] (Fig. 12) and also calculating the correct values of capacitance and resistance needed to supply the appropriated power to the stepper motor, by using (23), (24).

$$R \cong V_S / I_p \quad (23)$$

$$C = I_p / (dV / dt) \quad (24)$$

Where:

R is the value of the resistances R_9 and R_{10} (Fig.10)

C is the value of the capacitances C_{15} and C_{16} (Fig.10)

V_S is the maximum supply voltage foreseen on the application.

I_p is the peak of the load current.

dV/dt is the limit rise of the output voltage (200V/ μ s is generally used).

The result obtained with these calculus considering as value of V_S 9V and as I_P 3A, were a resistance value of R9 and R10 of 3 ohms, but was used one resistance of 2.7 ohms (Fig. 10), because, incrementing the max peak of load current tolerable by the L6203 at 3.33A, will be getting an excellent range of security because the nominal current of the motor is 1.4A/phase.

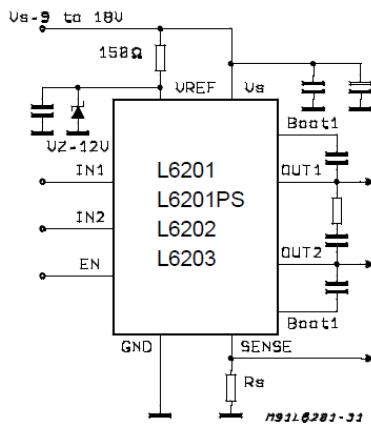


Fig.12. L6201/1P/2/3 Used at a Supply Voltage Range Between 9 and 18V (courtesy of SGS-THOMSON Microelectronics).

5 Programming part

5.1 Microcontroller functions

In order to make that the system works, the microcontroller needs to be programmed appropriately. Into the program the main characteristics of control were configured, e.g. the input and the output pins.

To programming the microcontroller first was built the principal structure of the elemental actions that the PIC will be executes, this tasks are:

- Starting the system putting the TS in the home position.
- Waiting by the Telemeter finishes scanning the present line.
- Moving the TS at the next position
- Repeating the last two points
- Identifying if the user change the parameters of scanning.
- Make the necessary adjusts, with base on the commands received from the user.

These principal tasks were the base in where the flowchart of the programming and the main program, are supported. One of the first actions before programming the microcontroller were build one flowchart (Fig. 13).

A second point to resolve, was determine the hardware configuration in the microcontroller, that

is, define how the pins will be working, this point was made with base on one part of the project, the electronic design, because with this is easy to know which element will be controller for which pin and which will be the necessary configuration for that pin.

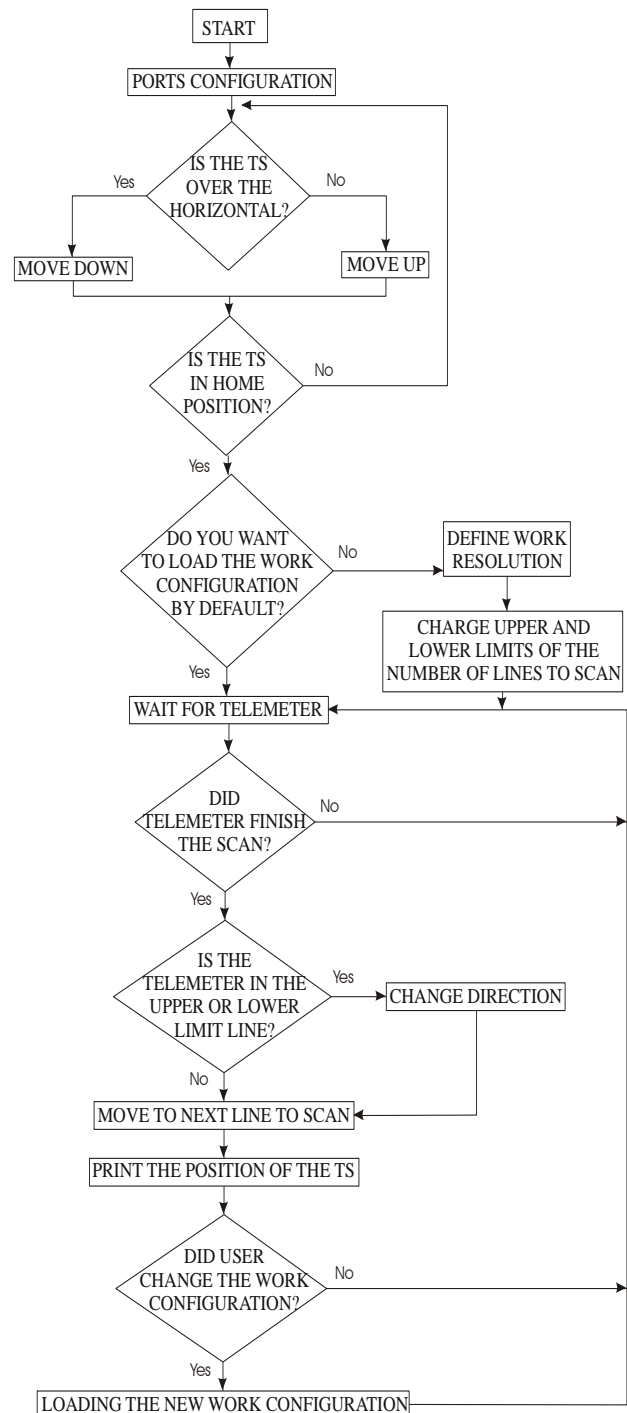


Fig. 13 Flowchart that represent the general function of the PIC16F870 and the PIC18F2455 working in the TS.

We are using RB0-RB4 pins as digital outputs and RB5- RB6 as digital inputs in port B of the PIC16F870. Besides RC1 is a digital output in port

C, port that also was configured to permit the communication via RS232 where RC7 is RX and the RC6 is TX. Detailed use of each pin is showed in Table V.

The microcontroller was programmed to communicate with a host computer via RS232 serial port, whereby the microcontroller receives characters strings that are commands or sends characters strings to indicate the state of the system and the actual position respect the horizontal.

TABLE V

Function assigned at the pins of the PIC16F87670

No. Pin	Name of Pin	Function designed
12	RC1/T10SCI	Pulse to the "clock-in" pin on L297 that produce the next step.
17	RC6/TX/CK	Transmission of serial data.
18	RC7/RX/DT	Reception of serial data.
21	RB0/INT	At low state reset the stepper motor controller. On low state full step work is selected, on high state half step work is selected.
22	RB1	
23	RB2	Change the direction CW/CCW
24	RB3/PGM	Enable/disable the power on the motor.
25	RB4	Define where the inhibit control currents will act, it's connected to the "ctrl" pin on L297.
26	RB5	Input to detect when the stepper motor controller is in home (outputs to motor in 0101).
27	RB6/PGC	Input to detect when the telemeter is on the horizontal.

A high level program (written in Java) is used to control the mechanism and acquire range data to compose 3D images.

The system has a default configuration, where the stepper motor moves at half steps and may give 180 range data lines in a whole frame of 64.8°. This configuration may be changed by the user to get more or less data lines to up and down respect the horizontal (maximum 126 range data lines per half frame), and the angular resolution may also be modified at 0.72° or 0.36° between the data lines.

The system recognizes 10 commands in ASCII code as shown:

{r} = homing of the mechanism.

{n} = in the settings means to leave the default values.

{y} = in the settings means to change the value of the settings as scan's limits and motor's step. In principal operation permits a continuous scan changing automatically the motor's direction on the limits.

{f} = changes at full step the resolution of the motor.

{h} = changes at half step the resolution of the motor.

{+} = in the settings permits increase the value of the upper limit or lower limit.

{-} = in the settings permits decrease the value of the upper limit or lower limit.

{space bar} = acceptance of the assigned limit values.

{2} = in principal operation, moves the telemeter upwards

{8} = in principal operation, moves the telemeter downwards.

6 Conclusions and Results

After making the necessary settings in all the system with different conditions of work, we obtained the first 3D image (Fig. 14) with a resolution of 0.36° and 64.8° frame field of view (180 range data lines), using the software designed by another lab student.

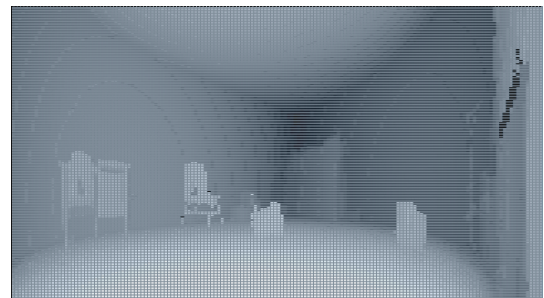


Fig. 14 Photo and 3D image of the laboratory obtained with the developed system (Courtesy of F. Bucio, Tech. Institute of Toluca).

Also all the devices were adapted to have an easy connection and use, for example the PCB were mounted into one acrylic box with its respective connector to the power supply cable, serial cable,

and the motor cable, all with the objective to do one handy device.

Moreover the interface of the control was designed to be used with the most common software or with most of the software developed to acquire 3D images, sending different messages that indicate the command that is needed to continue working and the state of the system, for example when the TS is putted on one new line, the microcontroller sends one message with the format (Fig. 15):

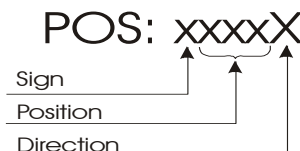


Fig. 15. Message of position sent by the microcontroller; the sign indicate if the TS is over (+) or under (-) the horizontal; the position indicate the present position of the TS; the direction indicates the present direction in which the TS is moved up or down (U/D).

The maximum speed obtained in the scan of a whole frame was around 4.8 minutes, this speed could be enhanced making an exactly coordination of the system between the telemeter, microcontroller and host computer, processing the data image with an efficient method, but even so the max speed only could be not less than 7s per frame scan with 252 range data lines, because the telemeter and the microcontroller need at least 13ms to scan a line and 0.5ms to move the telemeter to the next position, respectively. Besides, the necessary time to let the computer process input data coming from the TS and the LMS200 must be equal to the time required by them.

Home position is detected by means of the use of a microswitch; this method could be improved using an optical sensor or an inclinometer.

The current position of the mechanism is determined by means of the number of steps realized from the home position; to improve this information an absolute optical sensor could be used.

The TS can move up to 150 degrees/seg but the transmission of data from the LMS200 limits this operation, thus, at a speed of transmission of 9,600 bauds, working frequency by default of the LMS200. Working in this way, an image is obtained every 4,8 minutes. The LMS200 allows maximum speed transference 38,600 bauds, which would reduce transference time to a quarter of the current time. Additionally, the change to a strategy of type pipeline would allow improving this performance still more.

To finish this work, at the present the whole system which is mounted on the Pioneer 3-AT mobile robot (Fig. 16) is working fine and it is being used to make different tests to develop one new and better version of the software to acquire depth images of the robot's environment.

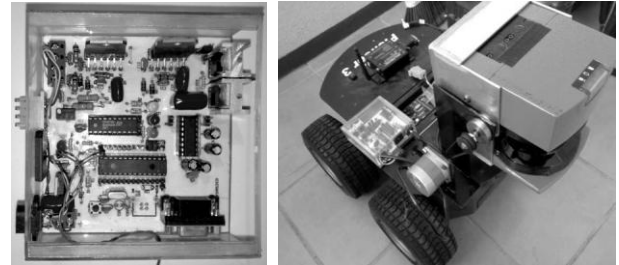


Fig. 16 In the left the PCB designed to control the TS and in the right the TS mounted on the Pioneer 3AT mobile robot.

Acknowledgments:

This work was supported mainly by the CONACyT (Mexico) under the agreement CO-028, and in part by the National Institute of Nuclear Research (ININ) and the Technological Institute of Toluca.

References:

- [1] Kay Boehnke, *Fast Object Localization With Real Time 3D Laser Range Sensor Simulation*, WSEAS TRANSACTIONS on ELECTRONICS, Issue 3, Volume 5, March 2008, ISSN: 1109-9445.
- [2] Hartmut Surmann, Kai Lingemann, Andreas N'uchter and Joachim Hertzberg, *A 3D laser range finder for autonomous mobile robots*, Proceedings of the 32nd ISR (International Symposium on Robotics), pp. 153 - 158, 19-21 April 2001.
- [3] Zhiyu Xiang and Wenhui Zhou, *3D Map Building for Mobile Robots Using a 3D Laser Range Finder*, D.-S. Huang, K. Li, and G.W. Irwin (Eds.): ICIC 2006, LNCIS 345, pp. 785 - 790, 2006. © Springer-Verlag Berlin Heidelberg 2006.
- [4] I Jivet, A Brindusescu, and I Bogdanov, *A Perception Oriented Formal Model for 3D Sensor Depth Images*, 12th WSEAS International Conference on SYSTEMS, Heraklion, Greece, July 22-24, 2008, ISBN: 978-960-6766-83-1, ISSN: 1790-2769.
- [5] Marius Ottesteanu and Vasile Gui, *3D Image Sensors, an Overview*, WSEAS TRANSACTIONS on ELECTRONICS, Issue 3, Volume 5, March 2008, ISSN: 1109-9445.

- [6] SICK *Technical Description Laser Measurement Systems LMS200 to LMS291*, © SICK AG · Division Auto Ident · Germany · All rights reserved 8008970/QI72/2006-12.
- [7] <https://www.mysick.com/eCat.aspx?go=Finder&Cat=Row&At=Fa&Cult=English&Category=Produktfinder>.
- [8] R. C. Hibbeler, *Engineering Mechanics Statics*, 10th ed., Mexico, published by Pearson Education, Inc., publishing as PRENTICE HALL, INC., 2004 pp. 437–490.
- [9] Theodore Baumeister, Eugene A. Avallone, Theodore Baumeister III, *Marks' Standard Handbook for Mechanical Engineers*, 8th ed., Ed. U.S.A. McGraw-Hill, 1978, Chapter 1 and 3.
- [10] Ferdinand P. Beer, E. Russell Johnston, Jr., *Vector Mechanics for Engineers: Dynamics*, 2th ed., Ed. Mexico: McGraw-Hill Inc., 1972.
- [11] R. C. Hibbeler, *Engineering Mechanics Dynamics* 10th ed., Mexico, published by Pearson Education, Inc., publishing as PRENTICE HALL, INC., 2004.
- [12] Fernando E. Valdes Perez, Ramon Pallas Areny, *Microcontrollers: Foundations and applications with PIC*, 1st ed., Ed. Alfaomega, 2007 Mexico.
- [13] Gilberto Mercado Lopez, *Design and Construction of robots*, published by Control Robotics and Automation (CRYA).
- [14] H. Sax, *Steeper motor driving - application note*, published by SGS Thomson Microelectronics, 1995.
- [15] Microchip, *PIC16F870/871 Data Sheet 28/40-Pin, 8-Bit CMOS FLASH Microcontrollers*, DS30569B, ©2003 Microchip Technology Inc.
- [16] Microchip, *PIC18F2455/2550/4455/4550 Data Sheet 28/40/44-Pin, High Performance, Enhanced Flash, USB Microcontrollers with nanoWatt Technology*, DS39632D, © 2007 Microchip Technology Inc.
- [17] Datasheet *L297-L297D, Stepper motor controller*, published by SGS Thomson Microelectronics, 1996.
- [18] Datasheet *L6201, L6202 - L6203 DMOS full bridge drive*, published by SGS Thomson Microelectronics, 1997.
- [19] I. Jivet, A. Brindusescu, *Real Time Representation of 3D Sensor Depth Images*, WSEAS TRANSACTIONS on ELECTRONICS, Issue 3, Volume 5, March 2008, ISSN: 1109-9445.
- [20] C. H. Jensen, *Engineering Drawing and Design*, 1st ed., Ed. U.S.A., McGraw-Hill Inc., 1968.
- [21] Hamilton H. Mabie, Charles F. Reinholtz, *Mechanisms and Dynamics of Machinery* 2th ed., Ed Limusa, 2004, Mexico.